International Journal of Electrical and Computer Engineering (IJECE)
Vol. 16, No. 1, February 2026, pp. 135~148
ISSN: 2088-8708, DOI: 10.11591/ijece.v16i1.pp135-148

Study on the acceleration process of three-phase induction motors driving elevator loads

Do Van Can, Phan Gia Tri
Faculty of Engineering and Technology, Quy Nhon University, Binh Dinh Province, Vietnam

Article Info

Article history:

Received May 2, 2025
Revised Sep 26, 2025
Accepted Nov 23, 2025

Keywords:

Acceleration process
Elevator drive system
Field programmable gate array
S-curve profile
Three phase motor

ABSTRACT

Three-phase induction motor drive systems, especially in elevator applications and other precision motion systems, require optimized acceleration profiles to minimize vibrations and extend mechanical lifespan. Previous studies have primarily focused on fast speed response control but often overlooked the impact of jerk, which affects smoothness and operational safety. This paper proposes a combination of field-oriented control (FOC) and S-curve acceleration profiles to reduce jerk and improve motion quality. A dynamic model of the drive system is developed to simulate the acceleration process, demonstrating that the S-curve significantly reduces torque and current oscillations, thus enhancing stability. The S-curve trajectory generation algorithm is implemented and deployed on a field programmable gate array (FPGA) hardware platform. Experimental hardware results confirm that the generated speed control signals possess high resolution and fast response, making the method suitable for embedded control systems in elevator drives and other sensitive motion-control applications. This integrated approach not only addresses the limitations of previous methods but also provides a practical solution to improve comfort, safety, and durability in various electromechanical drive systems.

Corresponding Author:

Do Van Can
Faculty of Engineering and Technology, Quy Nhon University
170 An Duong Vuong Street, Quy Nhon City, Binh Dinh Province, Vietnam
Email: dovancan@qnu.edu.vn

1. INTRODUCTION

The acceleration process of a three-phase induction motor plays a pivotal role in determining the performance, energy efficiency, and passenger comfort of elevator systems. Inappropriate acceleration either too slow or too abrupt can lead to mechanical stress, reduced lifespan of components, and uncomfortable experiences, particularly for sensitive users such as the elderly and children. Hence, optimizing the acceleration strategy is not only essential for system reliability but also for ensuring safety and ride quality.

Conventional elevator systems often rely on linear acceleration profiles, which are simple to implement but inherently introduce high levels of jerk at the transition points. This results in undesirable vibrations, noise, and mechanical wear, degrading the overall performance of the drive system. In contrast, S-curve acceleration profiles provide a smooth transition by limiting jerk and allowing gradual changes in acceleration, thereby offering superior ride comfort and mechanical stability—an increasingly crucial demand in modern vertical transportation.

Rotor flux-oriented control (FOC) has been extensively studied and applied to ensure fast system stabilization and minimal tracking error under variations in motor parameters, load conditions, and external disturbances [1], [2]. However, these studies primarily focus on control performance and pay insufficient

attention to motion quality, particularly the limitation of jerk in applications that demand high ride comfort, such as elevators. In [1] and [2], FOC is typically combined with linear acceleration profiles, which, although achieving fast dynamic response, generate high jerk levels at transition points. This results in vibrations, noise, and a negative user experience highlighting a limitation that must be addressed in modern elevator systems.

Field-oriented control (FOC) and direct torque control (DTC) are the two most widely adopted vector control strategies in electric motor drive systems [3]. FOC employs linear controllers in combination with pulse-width modulation (PWM) to control the stator voltage components [4], [5], while DTC uses a nonlinear approach to directly generate voltage vectors without modulators [6]. Studies such as [7], [8] have analyzed the advantages and disadvantages of these two methods across several criteria, including control characteristics, dynamic performance, parameter sensitivity, and implementation complexity, for both induction motors (IMs) and permanent magnet synchronous motors (PMSMs).

However, most of these studies focus primarily on control performance, fast dynamic response, and system stability, while neglecting motion quality especially the impact of jerk during acceleration and deceleration phases. This becomes a significant limitation in applications requiring high levels of smoothness and safety, such as elevator drive systems, where abrupt speed changes can lead to vibration, mechanical wear, and reduced user comfort.

Previous studies have applied intelligent control methods such as artificial neural networks (ANN) [9] and recurrent fuzzy neural networks (RFNN) [10] to improve adaptability and compensate for parameter uncertainties in AC motor control. While these approaches enhance dynamic response and stability, they focus primarily on regulation performance and do not consider jerk suppression or smooth motion planning, which are critical in applications like elevator systems. This paper addresses that gap by integrating jerk-limited S-curve profiles into the control strategy to improve ride comfort and mechanical stability.

Previous works have mainly emphasized fast response in motor control but overlooked the issue of jerk, which becomes critical in elevator load applications. Although S-curve acceleration profiles have been widely applied in stepper and servo motor systems to reduce vibration and enhance positioning accuracy [11], [12], these solutions are often constrained by the limited computational capabilities of stepper controllers and are rarely extended to induction motor drives. Studies [13], [14] have shown that optimizing acceleration and deceleration phases can significantly improve motion stability and reduce mechanical stress. However, these techniques have yet to be adapted for high-inertia, real-time applications like elevators. This study addresses that gap by applying high-order S-curve profiles to three-phase induction motors under FOC, aiming to ensure both motion smoothness and system responsiveness.

Several studies have focused on advanced control strategies for electric drives. For example, [15], [16] proposed an adaptive controller using feedback error learning (FEL) that combines a proportional integral derivative (PID)-based feedback loop with an intelligent feedforward controller to improve tracking and system stability. In parallel, motion control in servo [17] and stepper motors [18] has been studied for precision applications like camera positioning, emphasizing smooth acceleration to avoid vibration and positional errors. In elevator systems, where induction motors must deliver both precise stopping and high comfort [19], variable-speed drives have become essential to handle frequent starts and stops while ensuring smooth and safe travel [20], [21]. Although recent works have proposed jerk-reduction strategies for elevator drives, many are based on simplified models or lab-scale setups that lack compatibility with real-world elevator requirements [21].

Thus, existing research trends fall into two main streams: i) advanced control techniques for induction motors that prioritize speed tracking but often ignore jerk effects; and ii) S-curve acceleration planning that successfully limits jerk in servo or stepper motor applications [22], [23], but has seen limited adoption in full-scale induction motor elevator systems. This study aims to bridge that gap by integrating high-order S-curve acceleration into FOC for three-phase induction motors, enabling both smooth motion and fast dynamic response.

Not only elevator loads but also most drives powered by induction motors require a smooth start-up process to reduce vibration, noise, and extend equipment lifespan. This study addresses the gap between fast-response vector control strategies and the need for jerk-limited motion planning by proposing a method that combines FOC with high-order S-curve acceleration profiles. The proposed approach ensures smooth and stable acceleration while maintaining fast dynamic response and high energy efficiency. It is suitable for practical implementation in modern drive systems, particularly in vertical transportation applications such as elevators.

2. METHOD

2.1. Kinematic model of the elevator system

The elevator drive system comprises key mechanical components, including a three-phase induction motor, gearbox, traction pulley, steel cables, counterweight, and cabin. Its operation is significantly

influenced by unbalanced loading, mechanical friction, and the system's total moment of inertia, resulting in nonlinear dynamic behavior during acceleration and deceleration. For modeling and simulation purposes, the mechanical structure is simplified to an equivalent load mass referred to the motor shaft. The system's motion dynamics are governed by the following (1) [6]:

$$J_{eq} \cdot \frac{d\omega}{dt} = M_m - M_f \quad (1)$$

where J_{eq} is equivalent moment of inertia referred to the motor shaft (kg·m²); ω is angular velocity of the motor shaft (rad/s); M_m is motor-generated torque (Nm); M_f is load torque (including friction, load gravity, and inertia)

The load torque is calculated as (2):

$$M_f = r.(m_{eq}.g + F_{ms}) \quad (2)$$

where r is the radius of the traction pulley; F_{ms} is the total static friction force.

In a velocity control system, this model is used to determine the relationship between motor torque, rotational speed, and load at each point during the motion cycle. The three-phase induction motor used in elevator systems is typically of the squirrel-cage rotor type, controlled by a three-phase inverter that adjusts both frequency and voltage supplied to the motor.

The electromagnetic model of the induction motor is represented in the dq reference frame (rotor flux-oriented), which simplifies torque and speed control when using a variable frequency drive (VFD). The fundamental equations in this model are expressed as follows [24]:

$$\begin{cases} v_d = R_s i_d + \frac{d\psi_d}{dt} - \omega_e \psi_q \\ v_q = R_s i_q + \frac{d\psi_q}{dt} - \omega_e \psi_d \\ \psi_d = L_d i_d + L_m i_{dr} \\ \psi_q = L_q i_q + L_m i_{qr} \end{cases} \quad (3)$$

where i_d, i_q are components of stator current in the dq reference frame (A); v_d, v_q are stator voltages in the dq reference frame (V); ψ_d, ψ_q are d–q axis flux linkages (Wb); ω is electrical angular speed (rad/s); R_s is stator resistance (Ω); L_d is the inductance (H).

In system-level simulations, a parameterized model based on the drive characteristics described in (1) and (3) can be used. The electromagnetic torque $M_m(t)$ can be assigned directly by a PID controller or generated from a motion profile block based on the input profile, such as a linear acceleration profile. The inverter is a device that controls the voltage and frequency supplied to the induction motor, allowing precise adjustment of the motor's rotational speed. In elevator systems, accurate speed control is essential to ensure that the cabin stops precisely at the correct floor, provides smooth motion during starting and stopping, and remains stable under varying load conditions.

In this study, a novel control strategy is proposed that integrates field-oriented control (FOC) with an S-curve acceleration trajectory. This combined approach aims to reduce jerk, improve ride comfort, and enhance dynamic performance key requirements for elevator systems and other high-precision motion applications.

2.2. Proposed acceleration algorithm for motor based on S-Curve profile

The jerk equation (5) characterizes the rate of change of acceleration, which directly affects the quality of motor acceleration in elevator applications.

$$j(t) = \frac{da(t)}{dt} \quad (4)$$

The standard form of this Profile divides the motion into seven segments, ensuring that acceleration changes continuously in Figure 1: Jerk increases to j_{max}, acceleration increases to a_{max}, Jerk decreases to 0 → velocity is maintained.

Negative jerk decreases to $-j_{max}$, acceleration decreases to 0→ prepares for stopping. The design method for the S-curve Profile involves determining the number of motion segments based on a predefined motion pattern [25]. Then, the connection times between segments are calculated to ensure smooth transitions. Therefore, for a generalized S-curve Profile model, the total number of motion segments is given

by 2^{n-1}. Consequently, the number of transition points that need to be calculated is 2^n. The problem definition for the algorithm is as Figure 2:

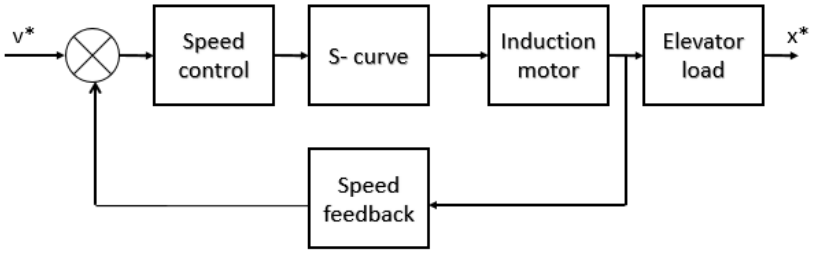

Figure 1. Speed control model with integrated S-Curve acceleration profile

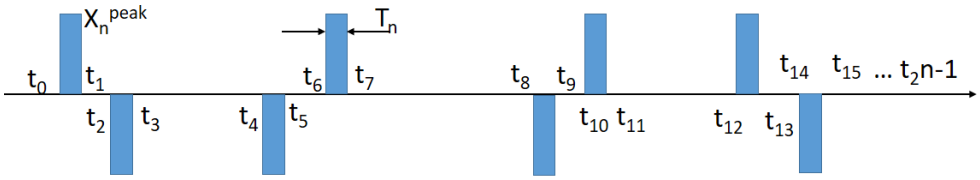

Figure 2. Template of the nth-order S-curve profile model

Input: The maximum allowable values of kinematic characteristics such as X_0^{peak}, X_1^{peak}, X_2^{peak}… X_n^{peak}. The goal is to design a smooth polynomial S-curve profile with a finite support such that these maximum values are not exceeded. Based on the definition of the generalized S-curve profile model, its kinematic features can be indirectly determined as follows. It should be noted that t_k represents the transition time between the k and (k+1) segments of the profile, while τ_k denotes the duration of a constant control input in the X_i^{peak} defined as follows [26]:

$$X_0^{peak} = \frac{X_n^{peak}}{2^n}\prod_{i=1}^{n}\left(t_{2^i-1} - t_0 + T_{n+1-i}\right) = \frac{X_n^{peak}}{2^n}\prod_{i=1}^{n}\left[\left(\sum_{j=0}^{i-1} 2^{\,j} T_{n+1-i+j}\right) + T_{n+1-i}\right] \quad (5)$$

Similarly,

$$X_1^{peak} = \frac{X_n^{peak}}{2^{n-1}}\prod_{i=1}^{n-1}\left[\left(\sum_{j=0}^{i-1} 2^j T_{n+1-i+j}\right) + T_{n+1-i}\right] \quad (6)$$

$$X_k^{peak} = \frac{X_n^{peak}}{2^{n-k}}\prod_{i=1}^{n-k}\left[\left(\sum_{j=0}^{i-1} 2^j T_{n+1-i+j}\right) + T_{n+1-i}\right] \quad (7)$$

$$X_{n-1}^{peak} = \frac{X_n^{peak}}{2}(t_1 - t_0 + T_n) = X_n T_n \quad (8)$$

Algorithm: The main task of the algorithm is to compute T_p, the duration of the constant input phase X_p^{peak}. The pseudocode of the algorithm is presented Figure 3:

$$X_0 = \frac{X_n}{2^2}\prod_{i=1}^{n}\left[\left(\sum_{j=0}^{i-1} 2^j T_{n+1-i+j}\right) + T_{n+1-i}\right] \quad (9)$$

$$X_q^{max\frac{X_n}{2^{n-q}}\prod_{i=1}^{n-q}\left[\left(\sum_{j=0}^{i-1} 2^j T_{n+1-i+j}\right)+T_{n+1-i}\right]} \quad (10)$$

$$X_q^{peak} = \frac{X_n}{2^{n-q}}\prod_{i=1}^{n-q}\left[\left(\sum_{j=0}^{i-1} 2^j T_{n+1-i+j}\right) + T_{n+1-i}\right] \quad (11)$$

In the algorithm, all durations T_p are initially set to zero according to equation (9). The value of T_p is first estimated based on the peak value of the position (X_q^{peak}), as defined in (11). This value of T_p is then used to compute the maximum values of the kinematic characteristics X_q^{max} according to (10). These computed maximum values are then compared with the corresponding input peak values. If any computed maximum exceeds the input peak, it indicates that Tp is too large. In such case, T_p is recalculated using (11). This iterative process continues until none of the input peak limits are violated.

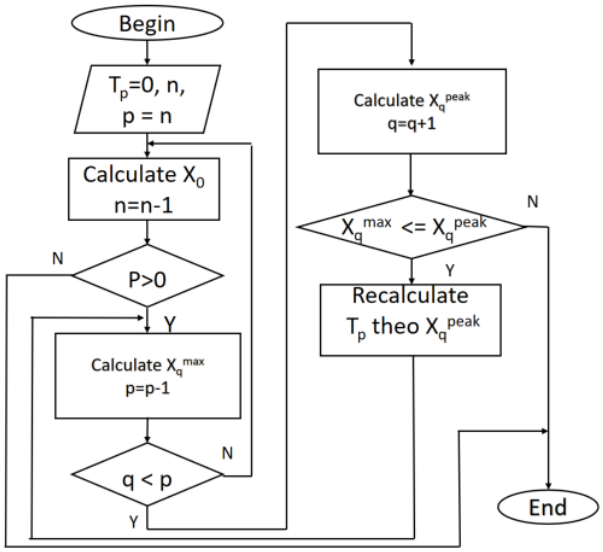

Figure 3. Flowchart: S-Curve profile generation algorithm

The S-curve algorithm, inherited from reference [26] is applied for the first time to the control of induction motors driving elevator loads. This represents a novel research direction, as no previous studies have implemented it, aiming to improve smooth acceleration and reduce vibrations during the startup process.

Compared to prior works, this algorithm stands out by:

- Being tailored for induction motor control, which has not been extensively addressed in existing S-curve research;
- Ensuring smooth torque generation, which minimizes current spikes and mechanical oscillation;
- Supporting hardware-level implementation on field programmable gate array (FPGA) for high-speed real-time operation, validated in this paper through both simulation and hardware-in-the-loop testing.

The combination of high smoothness, adaptability, and hardware feasibility makes the proposed algorithm a robust and practical solution for modern elevator drives and other industrial applications requiring precision and comfort.

2.3. Hardware implementation of acceleration and deceleration

Figure 4 illustrates the control circuit for S-curve acceleration/deceleration, implemented using a digital differential analyzer (DDA). Basic concept of S-curve acceleration/deceleration control: First, a series of pulses with a constant frequency Fi is generated by a pulse generator. The total number of generated pulses *N* determines the displacement during acceleration, while the frequency *Fi* defines the target speed. The control signal is obtained by subtracting the output of an accumulator from the pulse generator output, and this result is stored in register *p*. Simultaneously, the value of register *p(x)* and the accumulator output *y* are summed each time a pulse *Fa* is generated. The signal *Fa* is generated at fixed time intervals. Furthermore, the sum of the register value *x* and the accumulator output y is updated as follows: $y \leftarrow x+y$.

The FPGA hardware configuration is carefully designed to execute the control algorithm in real-time with high precision. The implementation on the DE1-SoC FPGA kit not only demonstrates the feasibility of the S-curve control algorithm for induction motors but also opens up practical applications in elevator control systems. The hardware architecture ensures real-time responsiveness and optimizes logic and memory resources, meeting the demands of industrial embedded systems.

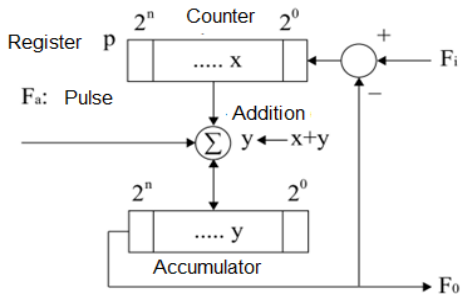

Figure 4. Hardware architecture for S-Curve acceleration/deceleration control

3. RESULTS AND DISCUSSION

3.1. Application scenario

Consider a three-phase squirrel-cage induction motor used in an elevator system in Table 1, controlled via a drive system consisting of an inverter and the motor itself. Suppose we intend to utilize a microcontroller integrated with the inverter for control implementation.

Table 1. Motor parameters used in simulation

Parameter	Value	Note
Rated voltage	380 V	Three-phase, star connection
Rated frequency	50 Hz	Vietnam/European standard
Rated power	2.2 kW	Suitable for elevator applications
Rated current	5.0 A	
Number of poles	4	Synchronous speed: 1500 rpm
Rated speed	1420 rpm	Slip ≈ 5.3%
Moment of inertia J	0.02 kg·m²	Includes elevator load
Stator resistance R_1	1.405 Ω	Measured from nameplate or test
Rotor resistance R_2 (referred to stator)	1.395 Ω	Converted to stator side
Stator inductance L_1	0.005839 H	
Rotor inductance L_2	0.005839 H	Assumed symmetrical
Magnetizing inductance L_m	0.1722 H	

3.2. Simulation and comparison of acceleration algorithms

In the context of high-performance drive systems such as elevators, the design of the acceleration profile plays a critical role in determining the smoothness, safety, and efficiency of motion. While conventional elevator systems typically rely on linear acceleration profiles for simplicity and ease of implementation, recent research efforts have attempted to improve ride quality and mechanical reliability by introducing advanced profiles such as parabolic, cubic, or polynomial-based strategies. However, these studies often overlook the impact of jerk dynamics a key factor affecting passenger comfort and component durability. To address this limitation, this paper proposes the implementation of a high-order S-curve acceleration profile integrated with FOC. This method is simulated and evaluated in detail, as illustrated in Figure 5, and compared against traditional linear acceleration approaches.

The velocity trajectory under the S-curve profile exhibits a smooth transition from 0 to approximately 148.6 rad/s within 1 second, forming a symmetric S-shaped curve. Unlike the constant-acceleration assumption used in many previous works [10], [13] which often results in sudden changes in velocity and torque, the S-curve method segments the motion into three distinct phases: increasing acceleration, constant acceleration, and decreasing acceleration. These smooth transitions are especially beneficial in elevator systems, where abrupt speed changes may cause discomfort or mechanical shocks. The acceleration profile (first derivative of velocity) in this study shows a continuous and bounded evolution, peaking at approximately 198.1 rad/s² and transitioning seamlessly across motion phases. In contrast, prior models [14] using linear or parabolic profiles often exhibit sharp slope changes or discontinuities at switching points, leading to mechanical stress accumulation over repeated cycles.

The jerk profile (second derivative of velocity) offers the most distinctive advantage of the proposed approach. Unlike traditional profiles that ignore or do not constrain jerk, the S-curve trajectory actively regulates jerk within ±990 rad/s³ throughout the motion phase. This control significantly reduces oscillations, enhances stability, and improves the service life of actuators aspects that were either underrepresented or absent in earlier control studies focused solely on torque tracking or speed error minimization.

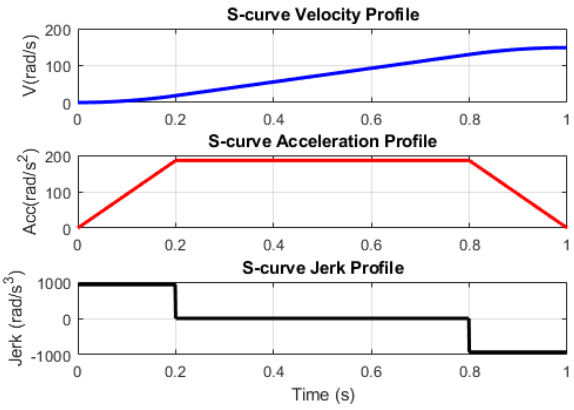

Figure 5. S-Curve acceleration profile chart

Furthermore, unlike many previous works that only validated their methods via MATLAB simulations or off-line tests, this study implements the entire motion profile generation algorithm on a real-time FPGA-based control platform, demonstrating not just feasibility but also practical deploy ability in embedded elevator drive systems. This hardware-in-the-loop capability highlights a major step forward compared to research limited to theoretical modeling.

In summary, simulation and analysis results clearly demonstrate that the high-order S-curve profile offers superior kinematic characteristics, including smoother transitions, reduced mechanical vibration, and improved dynamic response, when compared to traditional linear or polynomial acceleration schemes in the literature. The proposed strategy not only enhances passenger comfort but also improves energy efficiency and mechanical reliability—factors increasingly prioritized in modern elevator systems and industrial motion platforms such as collaborative robots and precision machining.

3.3. Analysis of motor speed control using the S-Curve

Figures 6 and 7 illustrate the acceleration, constant-speed, and deceleration phases of a three-phase induction motor controlled using a combined FOC and S-curve acceleration strategy. The simulation results show that the motor smoothly accelerates from 0 to 1420 rpm within 1 second, maintains that speed for the next 2 seconds, and decelerates back to zero by the 4th second. The speed trajectory follows a half-cosine shape without discontinuities, reflecting the smooth characteristics of the S-curve profile superior to traditional linear methods that often introduce abrupt transitions.

The electromagnetic torque increases steadily during the acceleration phase, peaking at approximately 15 Nm, and stabilizes at 5 Nm during constant-speed motion consistent with the physical relationship where torque is proportional to acceleration rather than speed. This smooth torque variation reduces mechanical stress and enhances drive system stability.

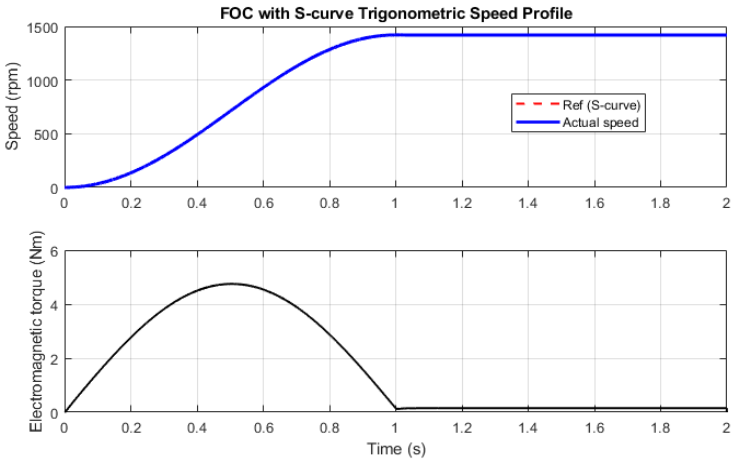

Figure 6. Motor speed and torque during S-Curve acceleration

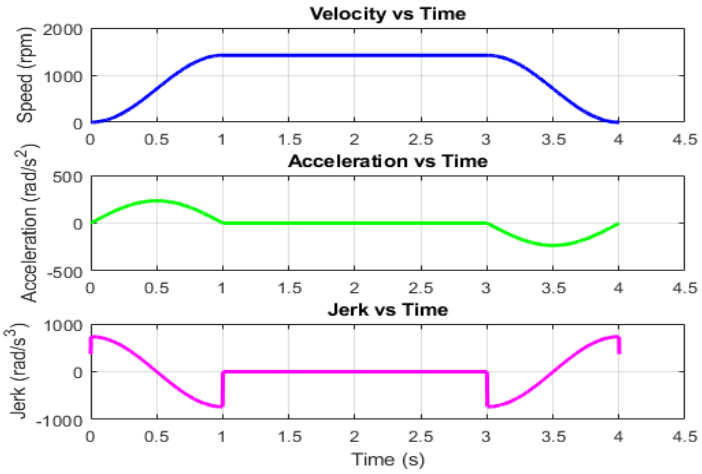

Figure 7. Startup of induction motor using S-Curve profile

Compared to previous studies, the proposed approach demonstrates significant improvements. In [8], the linear acceleration method failed to control jerk effectively, resulting in high impulsive forces and mechanical vibration. Our S-curve solution mitigates these issues by providing continuous jerk control. In [11], although FOC was implemented, the lack of integrated motion planning led to limited smoothness. Our method, combining FOC with S-curve planning, achieves comprehensive optimization of both speed control and kinematic performance. Moreover, while [25] presents a theoretical trajectory generation algorithm, it is not applied to induction motors with large inertia, such as elevator systems. In contrast, this study implements the algorithm on an FPGA-based platform, confirming its real-time feasibility and suitability for embedded applications.

In summary, Figures 6 and 7 validate that the proposed S-curve strategy enhances motion smoothness, minimizes mechanical shock, and extends the operational life of the system—making it ideal for applications requiring rapid yet gentle acceleration, such as elevators, cranes, and precision mechatronic systems.

3.4. FPGA implementation – experimental results

Initial parameters: System clock: 50 MHz (clock period = 20 ns), Output frequency: increases smoothly from ~1 kHz to ~30 kHz within 1 second, Update interval: every ~15–20 ms, one period value is updated. Simulation results from the s_curve_generator module demonstrate that the system successfully generates pulse signals with a gradually increasing frequency following an S-curve profile over a 1-second duration. The system was implemented in Verilog and simulated using ModelSim. Key model parameters include: A 50 MHz system clock a total of 20 S-curve steps (corresponding to an update interval of ~50 ms). Pulse period values ranging from 50,000 to 12,000 clock cycles (equivalent to 1 kHz to ~30 kHz).

Specifically, the output signal pulse_out is generated with an initial period of 50,000 clock cycles (which equals 1 kHz when the system clock is 50 MHz). After each predefined time interval (~20 ms), the period value is updated based on a lookup table (LUT) designed according to an S-curve profile. The period gradually decreases in steps not linearly but according to the characteristic S-curve shape, which enables smooth and progressive speed increases. The final pulse period reaches 12,000 clock cycles, corresponding to a frequency of approximately 4.17 kHz, and can be further increased if the LUT is extended.

The simulated (Figure 8) output signal `pulse_out` exhibits a smooth and continuously varying frequency profile, without any abrupt jumps typically seen in linear acceleration. This behavior is clearly observed in three distinct phases:

In the initial phase, the frequency increases slowly (positive jerk)
In the middle phase, the frequency increases steadily (constant acceleration)
In the final phase, the frequency increases more gradually (negative jerk)
This fully reflects the characteristic "S" shape of the S-curve Profile.
Acceleration time: 1 second
Frequency range: from 1 kHz to 30 kHz
Number of points: 64 samples generated according to the S-curve profile
Calculated parameters include: Frequency values (Hz), corresponding periods (μs)
Clock cycles per period based on a 50 MHz system clock (for use in LUTs in Verilog implementation)

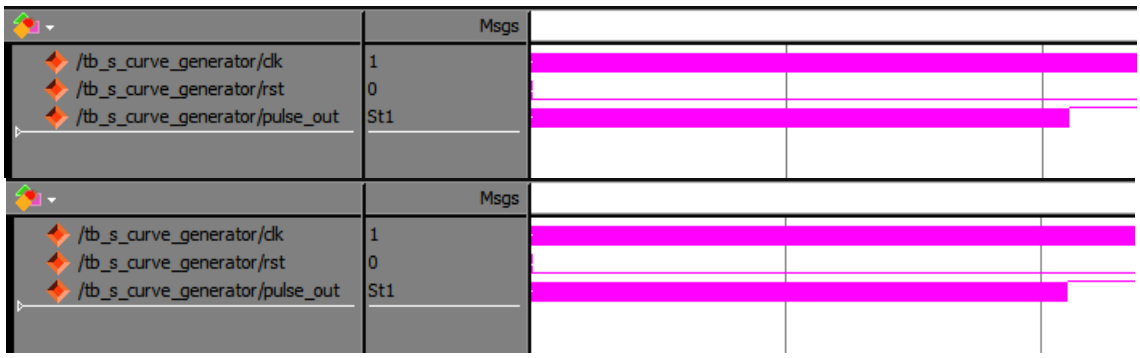

Figure 8. S-Curve acceleration process on the pulse output pin of the FPGA chip

Figure 9 shows both the frequency curve and the pulse period (clock cycles) over time presents a simulation of the S-curve acceleration profile, using 64 evenly distributed points over a total duration of 1 s (each sample spaced approximately 15.87 ms). The results demonstrate the system's ability to achieve precise and smooth speed control. Two main plots are shown: frequency vs. time and clock cycles per period vs. time, both reflecting the acceleration behavior of the motor control system under the S-curve approach.

Frequency Plot: The upper graph shows (Figure 9) the frequency increasing from 1,000 Hz at t = 0 s to 30,000 Hz at t = 1 s. Unlike linear acceleration, the frequency does not increase uniformly. Instead, it increases slowly at first, then more rapidly in the middle, and slows down again as it approaches the target frequency. The curve exhibits a symmetric half-cosine shape, characteristic of an S-curve profile that ensures controlled jerk during acceleration.

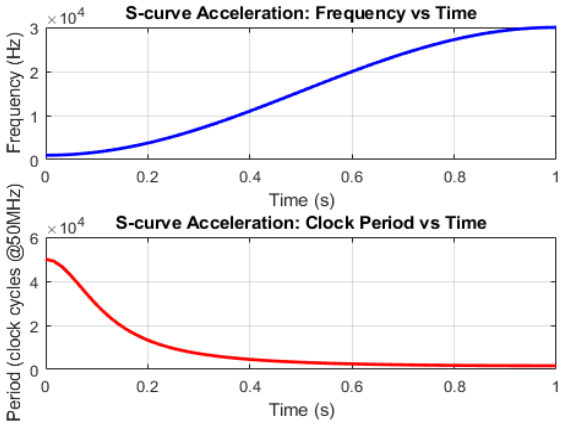

Figure 9. Frequency and period representation during S-Curve acceleration

3.4.1. Hardware Implementation on FPGA

The proposed method was experimentally validated using the DE1-SoC development board as shown in Figure 10. The experiments were conducted at the Chip Design Laboratory of Quy Nhon University to verify the feasibility and real-time performance of the trigonometric S-curve acceleration profile implemented in hardware. A Verilog-based implementation was developed to generate a one-shot PWM signal with a pulse width modulated according to the trigonometric S-curve trajectory. The design utilizes a counter to track time and a lookup table (LUT) stored in a memory-initialization file (.mif) to generate the desired amplitude profile. The PWM pulse is produced by comparing the LUT value with a continuously running counter, enabling smooth modulation of the pulse width. The system is programmed onto the DE1-SoC board (FPGA model 5CSEMA5F31), with the PWM output available on GPIO_0.

An extended version of the `top_scurve_pwm.v` module was developed to control six PWM channels (GPIO_0 to GPIO_5). These outputs represent three-phase motor signals (U, V, W) and their complementary signals (~U, ~V, ~W), with each phase shifted by one-third of a cycle. All channels use the same S-curve profile stored in ROM but are phase-shifted accordingly. The PWM switching frequency is set

at 1 kHz, and the duty cycle dynamically follows the trigonometric S-curve. After compilation and pin assignment, the design is downloaded to the FPGA board for real-time testing and waveform acquisition.

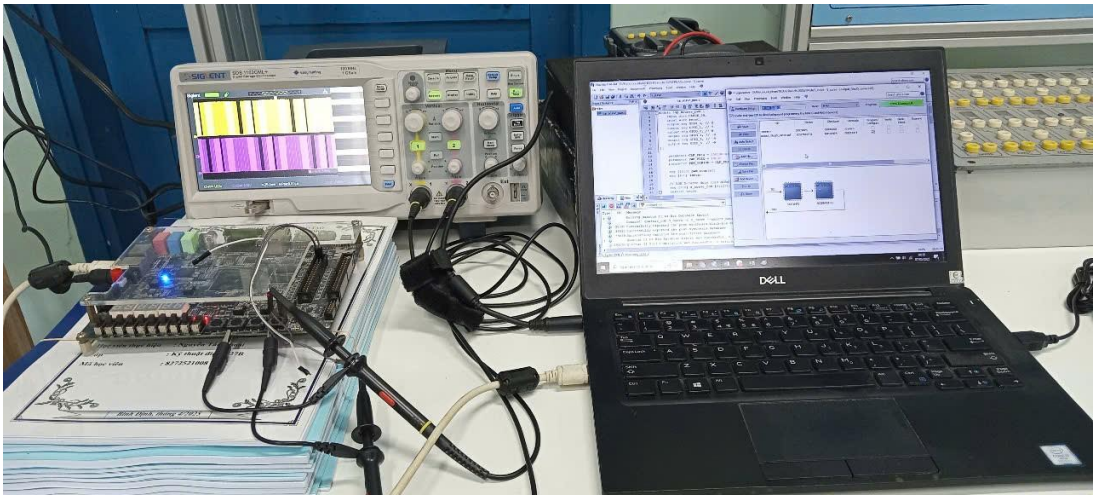

Figure 10. Experimental setup for trigonometric S-curve implementation on FPGA

The output PWM frequency remains stable at 1 kHz (Figure 11 is signals U, V), maintained by a precise counter synchronized to the 50 MHz system clock. This frequency is well-suited for controlling induction motors in applications that require smooth variations in speed and torque, such as elevators or cranes. The use of a sinusoidal/cosine-based S-curve trajectory enables smooth modulation of the PWM duty cycle, avoiding abrupt transitions. The duty cycle gradually increases from 0% to approximately 100% and then symmetrically decreases, forming a smooth acceleration-deceleration cycle. This approach helps limit current surges in the stator windings, reduce torque ripple, and mitigate mechanical shocks during transient phases.

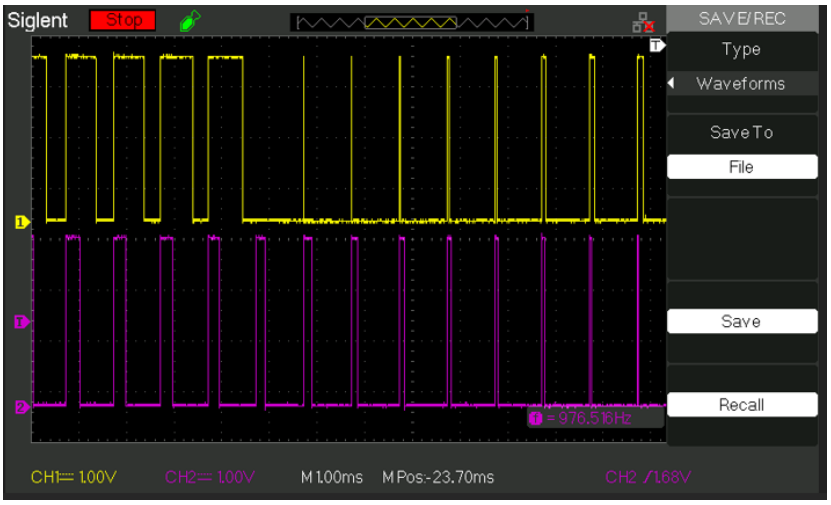

Figure 11. PWM waveform based on trigonometric S-curve profile

The three output channels (U, V, W) are phase-shifted by 120 electrical degrees, ensuring proper temporal distribution across phases and accurately reconstructing a balanced rotating magnetic field. The complementary channels (~U, ~V, ~W) provide inverted PWM signals for H-bridge or three-phase inverter configurations, enabling efficient bidirectional torque control. Figure 12 show the PWM waveform of phase U and its complementary signal; the remaining phases (V and W) exhibit similar behavior.

The sinusoidal/cosine-based S-curve PWM waveform is highly suitable for soft-start and soft-stop motor control, as it produces more linear torque characteristics and is particularly effective in systems where minimizing mechanical shocks or current oscillations during load transitions is critical. The application of the trigonometric S-curve trajectory in three-phase PWM modulation has yielded promising results in terms of waveform smoothness, frequency stability, and the ability to generate soft and continuous torque. This approach proves to be a practical and effective method for enhancing the performance and reliability of electric drive systems in precision motion control applications.

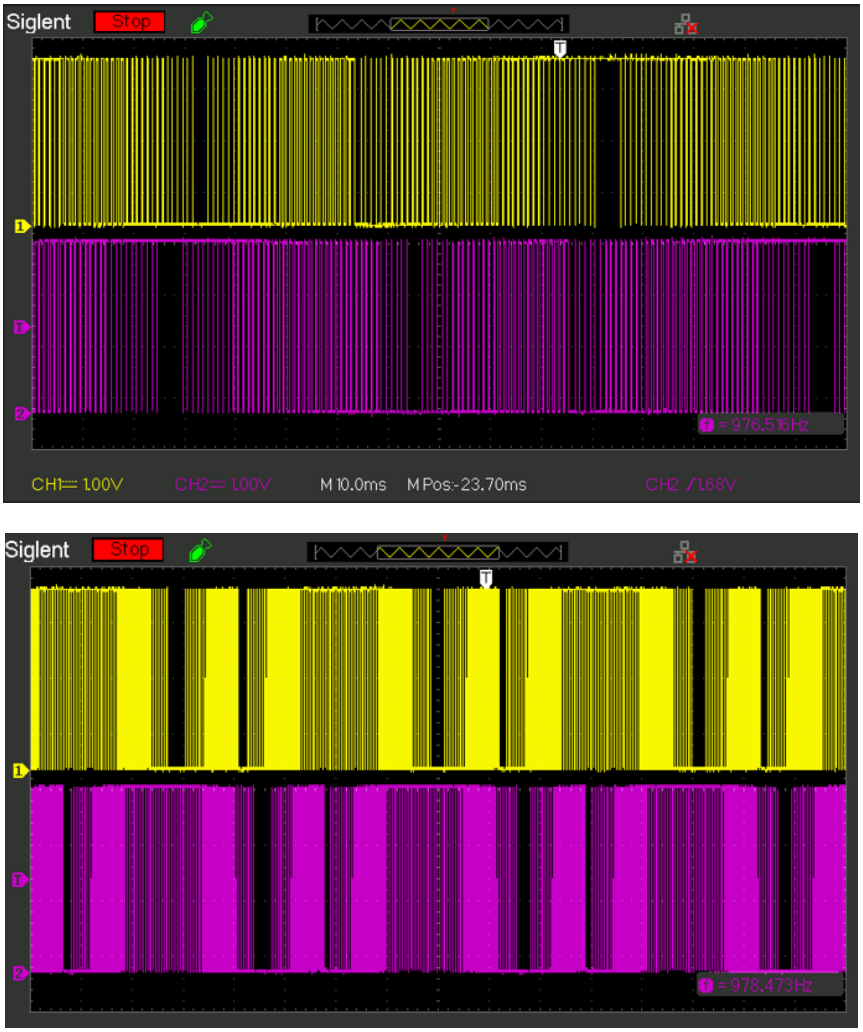

Figure 12. Measured PWM signals: phase U and its complementary output (~U)

Compared to [8], where the control system applies linear acceleration and shows significant overshoot, high jerk, and speed ripples during transient states, our method demonstrates superior smoothness and dynamic stability. In [11], although FOC is implemented, the trajectory generation is limited to basic ramp profiles, lacking jerk control, which causes mechanical stress in high-inertia systems. Meanwhile, [25] presents a theoretical multi-segment S-curve trajectory planner but does not apply it to real-time motor control or validate it on embedded platforms.

This paper addresses these gaps by not only applying a high-order S-curve algorithm tailored for motion planning but also implementing and testing it in real-time on an actual FPGA-based system. The results confirm that the control system is capable of generating high-resolution velocity references with fast response, smooth transition, and mechanical safety. This contribution highlights the practical feasibility and industrial applicability of integrating S-curve trajectories into embedded control for elevator systems especially in scenarios where ride comfort, precise floor-stopping, and extended actuator lifespan are critical.

4. CONCLUSION

This study aligns well with the scope of the journal, as it focuses on advanced control strategies for three-phase induction motors core components in modern industrial automation and drive systems. Specifically, it targets applications that demand smooth and safe motion, such as elevators, which fits the journal's direction toward intelligent control, embedded systems, and industrial drives. The objective of this research is to optimize the acceleration process by reducing jerk and torque oscillations.

The approach combines dynamic system modeling with a high-order S-curve motion planning algorithm, implemented both in simulation and hardware (FPGA), ensuring practical feasibility. The novelty lies in the development of a trajectory generation algorithm that considers jerk limits an aspect often overlooked or treated only theoretically in previous works. The FPGA-based implementation confirms its readiness for real-world embedded systems.

This paper contributes to existing knowledge by proposing a motion control solution that ensures smoother acceleration for induction motors, enhancing mechanical reliability and passenger comfort. It offers both theoretical insight and practical value. In the long term, the proposed method has potential for broader applications such as cranes, high-speed conveyors, robotic arms, and CNC platforms where precise and stable motion control is essential. Given its scientific value, practical applicability, and high scalability, the authors believe this paper deserves to be published and will serve as a useful reference for researchers and engineers in industrial drives and embedded motion control systems.

ACKNOWLEDGMENTS

The authors would like to express their sincere thanks to the faculty and staff of the Department of Electrical Engineering, Quy Nhon University, for their support during the research process. This study was conducted through simulation and experimental work at Laboratory 314, Quy Nhon University. The authors also gratefully acknowledge the individuals who provided technical assistance and valuable discussions that contributed to the success of this work.

FUNDING INFORMATION

Authors state no funding involved.

AUTHOR CONTRIBUTIONS STATEMENT

This journal uses the Contributor Roles Taxonomy (CRediT) to recognize individual author contributions, reduce authorship disputes, and facilitate collaboration.

Name of Author	C	M	So	Va	Fo	I	R	D	O	E	Vi	Su	P	Fu
Do Van Can	✓	✓	✓	✓	✓	✓	✓	✓	✓	✓	✓	✓	✓	
Phan Gia Tri		✓				✓		✓	✓	✓	✓	✓		

C : **C**onceptualization
M : **M**ethodology
So : **So**ftware
Va : **Va**lidation
Fo : **Fo**rmal analysis
I : **I**nvestigation
R : **R**esources
D : **D**ata Curation
O : Writing - **O**riginal Draft
E : Writing - Review & **E**diting
Vi : **Vi**sualization
Su : **Su**pervision
P : **P**roject administration
Fu : **Fu**nding acquisition

CONFLICT OF INTEREST STATEMENT

Authors state no conflict of interest.

INFORMED CONSENT

This study does not involve any human participants or identifiable personal data.

ETHICAL APPROVAL

This study does not involve human or animal subjects.

DATA AVAILABILITY

The data that support the findings of this study were measured and collected at Laboratory 314, Quy Nhon University. The data are available from the corresponding author upon reasonable request.

REFERENCES

[1] M. A. W. Begh and H. G. Herzog, "Comparison of field oriented controland direct torque control," *TechRxiv*, no. March 2018, pp. 1–16, 2018, doi: 10.36227/techrxiv.171332371.13141782/v1.

[2] M. Jannati, N. R. N. Idris, and M. J. A. Aziz, "Performance evaluation of the field-oriented control of star-connected 3-phase induction motor drives under stator winding open-circuit faults," *Journal of Power Electronics*, vol. 16, no. 3, pp. 982–993, May 2016, doi: 10.6113/JPE.2016.16.3.982.

[3] D. Pebrianti, O. Ying Peh, R. Samad, M. Mustafa, N. R.H Abdullah, and L. Bayuaji, "Intelligent control for visual servoing system," *Indonesian Journal of Electrical Engineering and Computer Science*, vol. 6, no. 1, p. 72, Apr. 2017, doi: 10.11591/ijeecs.v6.i1.pp72-79.

[4] G. Cimini, G. Ippoliti, G. Orlando, and M. Pirro, "PMSM control with power factor correction: Rapid prototyping scenario," *International Conference on Power Engineering, Energy and Electrical Drives*, no. May 2013, pp. 688–693, 2013, doi: 10.1109/PowerEng.2013.6635693.

[5] C. Klarenbach, J. Onno, and B. Str, "Fast and high precision motor control for high performance servo drives," *Cologne University of Applied Sciences, Betzdorfer Str. 2, 50679 Köln, Germany*, pp. 326–333, 2010.

[6] A. A. Ali, F. Ben Salem, and J. A. K. Mohammed, "Design of an electric elevator drive with high riding quality under jerk control," *Engineering, Technology and Applied Science Research*, vol. 14, no. 5, pp. 16438–16443, 2024, doi: 10.48084/etasr.8202.

[7] A. Chikhi, M. Djarallah, and K. Chikhi, "A comparative study of field-oriented control and direct-torque control of induction motors using an adaptive flux observer," *Serbian Journal of Electrical Engineering*, vol. 7, no. 1, pp. 41–55, 2010, doi: 10.2298/SJEE1001041C.

[8] D. Van Can, "Current controller design based on FPGA," *Journal of Science - Quy Nhon University*, vol. 15, no. 1, pp. 71–78, 2020.

[9] K. Sabahi, M. Teshnehlab, and M. A. Shoorhedeli, "Recurrent fuzzy neural network by using feedback error learning approaches for LFC in interconnected power system," *Energy Conversion and Management*, vol. 50, no. 4. pp. 938–946, 2009, doi: 10.1016/j.enconman.2008.12.028.

[10] D. H. D. Khoa, S. H. Thanh, and N. C. Ngon, "Intelligent control of induction motor using recurrent fuzzy neural networks," *TNU Journal of Science and Technology*, vol. 227, no. 08, pp. 46–55, 2022.

[11] B. Kumar, P. Wang, and A. S. Hossain, "Design of motion profile of stepper motor for elevator using Arduino Uno," *North American Academic Research Journal*, vol. 3, no. 04, pp. 683–695, 2020.

[12] A. Drumea, C. I. Marghescu, M. Pantazică, G. Jitianu, and A. Vlad, "S-curve motion control implementation using 32-bit microcontroller," in *Proceedings of 2022 International Conference on Hydraulics and Pneumatics - HERVEX November 9-10, Băile Govora, Romania*, 2022, no. 2, pp. 160–165.

[13] Z. Zhang and Y. Yu, "S-type speed control curve based on the number of pulses," *Journal of Physics: Conference Series*, vol. 2196, no. 1, 2022, doi: 10.1088/1742-6596/2196/1/012038.

[14] V. Kombarov, V. Sorokin, O. Fojtů, Y. Aksonov, and Y. Kryzhyvets, "S-curve algorithm of acceleration/deceleration with smoothly-limited jerk in high-speed equipment control tasks," *MM Science Journal*, vol. 2019, no. November, pp. 3264–3270, 2019, doi: 10.17973/MMSJ.2019_11_2019080.

[15] F. Allam, Z. Nossair, H. Gomma, I. Ibrahim, and M. Abdelsalam, "Evaluation of using a recurrent neural network (RNN) and a fuzzy logic controller (FLC) in closed loop system to regulate blood Glucose for Type-1 Diabetic Patients," *International Journal of Intelligent Systems and Applications*, vol. 4, no. 10, pp. 58–71, 2012, doi: 10.5815/ijisa.2012.10.07.

[16] P. Kumar and R. Mishra, "Implementation of FPGA based PID controller for DC motor speed control system," *International Journal of Engineering Trends and Technology*, vol. 4, no. 3, pp. 471–476, 2013.

[17] X. Li, "Optimizing S-curve Velocity for Motion Control," *Journal of Applied Mathematics*, no. FEBRUARY 2010, pp. 1–12, 2010.

[18] X. Wei, "Acceleration and deceleration control design of step motor based on TMS320F240," *Procedia Engineering Elsevier*, vol. 15, pp. 501–504, 2011, doi: 10.1016/j.proeng.2011.08.095.

[19] V. I. Vlachou, D. E. Efstathiou, and T. S. Karakatsanis, "Design, analysis and application of control techniques for driving a permanent magnet synchronous motor in an elevator system," *Machines*, vol. 12, no. 8, 2024, doi: 10.3390/machines12080560.

[20] R. Akçelik and M. Besley, "Acceleration and deceleration models," *Springer Series in Advanced Manufacturing*, no. January 2001, pp. 107–156, 2008, doi: 10.1007/978-1-84800-336-1_4.

[21] M. Osama and O. Abdul-Azim, "Implementation and performance analysis of an elevator electric motor drive system," *2008 12th International Middle East Power System Conference, MEPCON 2008*, pp. 114–118, 2008, doi: 10.1109/MEPCON.2008.4562368.

[22] C. Li and F. Chen, "Application of S-Curve acceleration and deceleration in winding of bond-wire," *International Journal of Trend in Research and Development*, vol. 8, no. 4, pp. 158–161, 2021.

[23] L. Wang and J. Cao, "A look-ahead and adaptive speed control algorithm for high-speed CNC equipment," *International Journal of Advanced Manufacturing Technology*, vol. 63, no. 5–8, pp. 705–717, 2012, doi: 10.1007/s00170-012-3924-7.

[24] R. Rahmatullah, N. F. O. Serteller, and V. Topuz, "Modeling and simulation of faulty induction motor in DQ reference frame using MATLAB/SIMULINK with MATLAB/GUIDE for educational purpose," *International Journal of Education and Information Technologies*, vol. 17, pp. 7–20, Mar. 2023, doi: 10.46300/9109.2023.17.2.

[25] K. D. Nguyen, T. C. Ng, and I. M. Chen, "On algorithms for planning S-Curve motion profiles," *International Journal of Advanced Robotic Systems*, vol. 5, no. 1, pp. 99–106, 2008, doi: 10.5772/5652.

[26] A. Gavai, A. Kasbekar, and A. V Mulay, "Position control of BLDC motor using S-Curve for trajectory planning and feedforward control design," in *2019 10th International Conference on Computing, Communication and Networking Technologies (ICCCNT), Kanpur, India,* 2019, pp. 1-6*,* doi: 10.1109/ICCCNT45670.2019.8944914.

BIOGRAPHIES OF AUTHORS

Do Van Can Born in 1981, received a master's degree in automation in 2009 and a Ph.D. degree in 2019 from the University of Danang. Since 2004, he has been a lecturer at the Faculty of Engineering and Technology, Quy Nhon University. His research interests include chip design, FPGA, SoC, electric machine control, CNC machine tools, industrial networks, and SCADA systems. Phone: +84 935 253 630. He can be contacted at email: dovancan@qnu.edu.vn.

Phan Gia Tri Born 1997, received the B.Eng. in electrical–electronics engineering from Quy Nhon University in 2019 and the M.Sc. in control engineering and automation from Ho Chi Minh City University of Technology, Vietnam National University–HCMC, in 2022. Since 2022, he has been with the Automation Division, Faculty of Engineering and Technology, Quy Nhon University, where he teaches and conducts research. His research interests include image processing and mobile robotics. Phone: +84 983 306 315. He can be contacted at email: phangiatri@qnu.edu.vn.